ELSEVIER

Journal of Power Sources 81–82 (1999) 661–665

JOURNAL OF POWER SOURCES

www.elsevier.com/locate/jpowsour

γ-MnO_2 for Li batteries
Part II. Some aspects of the lithium insertion process into γ-MnO_2 and electrochemically lithiated γ-Li_xMnO_2 compounds

S. Sarciaux *, A. Le Gal La Salle, A. Verbaere, Y. Piffard, D. Guyomard

Laboratoire de Chimie des Solides, Institut des Matériaux de Nantes, B.P. 32229, 44322 Nantes Cedex 3, France

Abstract

The first Li insertion into various γ-MnO_2 compounds, characterized by their rates of De Wolff and microtwinning defects, and the reversible Li intercalation process into the resulting γ-Li_xMnO_2 materials have been investigated. The first Li insertion into γ-MnO_2 is a first order reaction which occurs via a nucleation and growth mechanism. When the concentration of De Wolff defects increases, the thermodynamic potential of this reaction decreases and its kinetics becomes slower. The resulting γ-Li_xMnO_2 materials exhibit a very close structural relationship with so-called CDMO materials. The reversible Li intercalation process into γ-Li_xMnO_2 occurs in two steps that both operate via a two-phase mechanism. The concentration of De Wolff defects also plays a detrimental role in the kinetics of reversible lithium intercalation in electrochemically formed γ-Li_xMnO_2. Structural characterization of materials at the end of the first discharge have shown that γ-MnO_2 materials with a high rate of De Wolff defects are subjected to deeper structural rearrangements.

Keywords: γ-MnO_2; γ-Li_xMnO_2; Li insertion process; Thermodynamics; Kinetics; Structural changes

1. Introduction

The structure of γ-MnO_2 can be described as resulting mainly from two types of structural defects in a Ramsdellite structure: intergrowth of rutile-type structural units (Pr is the rutile concentration) and packing faults corresponding to microtwinning (Mt is the amount of microtwinning) [1–3].

γ-MnO_2 compounds are good candidates as the positive electrode for rechargeable lithium batteries, due to their high intercalation voltage, low cost of raw material and non-toxicity. Prior to this use, they must be dehydrated and after this treatment they are usually referred to as HTMD (Heat Treated Manganese Dioxides). Structural evolutions occurring during electrochemical insertion of lithium in γ-MnO_2 compounds have been studied by several authors [4–8]. However, it is quite difficult to compare all these previous results because of a lack of structural characterization of starting compounds and lithiated phases obtained after intercalation.

By heating γ-MnO_2 materials in air with a lithium salt at 300–400°C, lithiated MnO_2 materials, also called CDMO (Composite Dimensional Manganese Oxide), are obtained [8–13]. They correspond to a mixture between a majority phase, whose lithium content does not exceed 0.33 Li/Mn, and a minority phase of spinel type (and/or Li_2MnO_3). This mixture, with a Li:Mn ratio of 3:7, is considered to be a promising cathode material for rechargeable lithium batteries in view of its relatively high specific capacity and long-term cyclablity.

This paper is intended to characterize the lithium intercalation process (mechanism, kinetics and thermodynamic parameters) into γ-MnO_2 and γ-Li_xMnO_2 compounds. Different techniques have been used including: electrochemistry (cyclic voltammetry, chrono-amperometry, galvanostatic cycling) and simulation of X-ray diffraction patterns.

2. Experimental

Electrodeposited γ-MnO_2 (EMDs prepared according to the conditions described in a companion paper (see Part I) and HTMD materials (prepared from these EMDs and

* Corresponding author

0378-7753/99/$ - see front matter
PII: S0378-7753(98)00230-4

from a CMD (obtained from Sedema)), were used for the electrochemical studies. Their characterization in terms of physico-chemical parameters (y and n, in the general formulation MnO_y, nH_2O) and structural parameters (concentration of de Wolff defects Pr and amount of microtwinning Mt) is also described in Part I.

Electrochemical lithium insertion and cell cycling were performed in Swagelok test cells monitored by a Mac-Pile system in potentiodynamic and galvanostatic modes [14], using metallic lithium as the negative electrode. The positive electrode was prepared by deposing on 5–10 mg of a mixture (on an Al current collector) typically containing 85 wt.% of γ-MnO_2, carbon black and polyvinylidene fluoride (PVDF) being the other components of the composite electrode. A 1 M solution of $LiPF_6$ in ethylene carbonate (EC) and dimethyl carbonate (DMC) (75:25) was used as the electrolyte. Slow scan rates (20 mV/h) in potentiodynamic mode and C/6 rate in galvanostatic mode were used for electrochemical studies. To investigate the lithium insertion mechanism into γ-MnO_2, chrono-amperometric measurements were carried out. This principle consists of linearly varying the voltage with time, step by step and analysing the current evolution during every step. All voltages given in the text are reported vs. the reference Li^+/Li.

X-ray Diffraction (XRD) patterns were recorded on a Siemens D5000 diffractometer using Cu Kα radiation, and simulated with the use of the Diffax program [15].

3. Results and discussion

3.1. Electrochemical characterisation at the first insertion

3.1.1. Comparison of curves U–x between a γ-MnO_2 and a CDMO compound

Fig. 1a depicts the typical electrochemical intercalation behaviour of a HTMD sample with $y = 2$, during the first lithium insertion–deinsertion cycle. As already mentioned in Part I, it shows that a first order reaction (otherwise said a two-phase mechanism) occurs during the first discharge down to 2 V, leading to a new lithiated phase. During the second discharge, we clearly observe two distinct redox phenomena: the first one at about 3.4 V and the second at 3 V. This highlighted observation is a new result. In previously published works, capacity at 3.4 V was rarely utilised, consequently, low capacity and long-term cyclability were obtained, but with an important loss of capacity after the first cycle.

CDMO is electrochemically characterized (Fig. 1b) by two reversible redox phenomena: an insertion of lithium at 3 V during the first discharge, then a larger reversible process with two steps which take place at 3.4 and 3 V (at the following discharge). This gain of capacity, with an insertion process at about 3.4 V during the second discharge, is in agreement with the fact that chemically

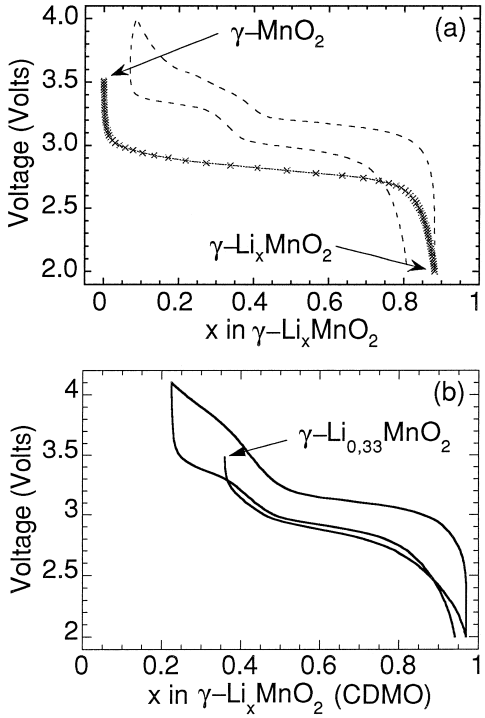

Fig. 1. Curve $U-x$ of (a) a γ-MnO_2 (Pr = 45%, Mt = 8%, $y = 2$) and (b) a CDMO compound, in the 2–4 V range, with a 20 mV/h scanning rate.

pre-inserted lithium can be extracted during the charge at 4 V and re-intercalated at about 3.4 V in reduction.

Electrochemical behaviors described in Fig. 1a (after the first discharge) and b show important similarities. This observation suggests a very close structural relationship between the lithiated phase obtained after the first Li insertion into a HTMD and a CDMO, as already mentioned in Ref. [8]. It was then decided to call γ-Li_xMnO_2 the electrochemically lithiated materials obtained from γ-MnO_2.

3.1.2. Insertion mechanism

Fig. 2 depicts a typical chrono-amperometric curve of the first lithium insertion in a γ-MnO_2. The curve shows many points corresponding to the current evolution during every voltage step. The whole set of points draws an asymmetric peak. The current increases (in absolute value) during some steps vs. time in the peak ascent. This behaviour of current is in agreement with a first order transformation [16].

The difference between the monitored voltage V and the initial voltage V_{onset} of the two-phase mechanism (thermodynamic potential) is the parameter which controls the insertion reaction rate. An increasing current, at constant voltage, means an increase of the overall transformation rate. If we assume that the current is constant per surface area unit of boundary phases because of a constant ($V - V_{onset}$) driving force, this increasing current can be interpreted as an increase of the surface area of the phase interface, such as by a nucleation and growth mechanism, i.e., a kind of initial adaptation of materials.

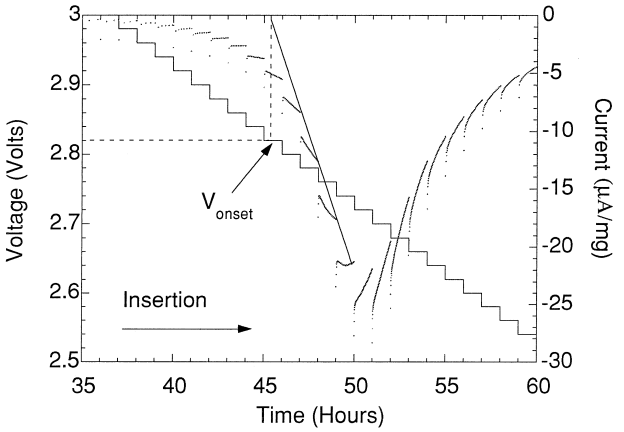

Fig. 2. Chrono-amperometric curve of a γ-MnO_2 (Pr = 97%, Mt = 3%, $y = 2$) during the first discharge, in the 2–4 V range and with a 20 mV/h scanning rate.

3.1.3. Thermodynamic study

The extrapolation from ascending linear I vs. V variation to zero current, from the chrono-amperometric curves, leads to the determination of the thermodynamic potential of the first order transformation γ-MnO_2/γ-Li_xMnO_2. Due to the nucleation and growth mechanism, the shape of the curves makes difficult to evaluate V_{onset} precisely because of increasing current at every voltage steps. However, qualitative measurements on various γ-MnO_2 samples show the effect of Pr to be significant as illustrated in Fig. 3. A continuous evolution of the V_{onset} voltage with Pr values is observed. The thermodynamic potential is much lower as Pr value increases. Consequently, the initial adaptation of materials, which contain many Pr defects, is more difficult. This result suggests that the transformation starts within the Ramsdellite units of the structure, which are thermodynamically more favourable than pyrolusite units. On the other hand, none regular variation with Mt values was noted.

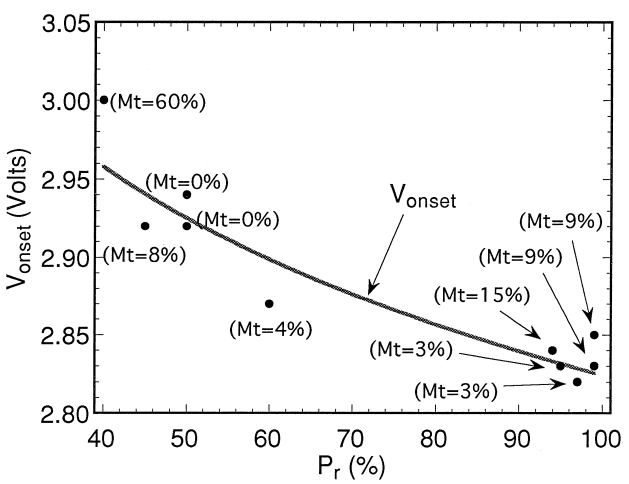

Fig. 3. Evolution of the thermodynamical voltage V_{onset} with Pr values, during the first discharge, with a 20 mV/h scanning rate.

Table 1
Influence of time on the lithium insertion capacity for the first discharge of two HTMD samples

Pr, Mt	Capacity (mA h/g)	
	Discharge in 6 h	Discharge in 100 h
45, 8	240	262
95, 3	182	260

3.1.4. Kinetics of the transformation

In order to evaluate the influence of Pr on the kinetics, we examined the effect of a large change of discharge time on the first lithium insertion capacity into HTMD samples with similar physico-chemical parameters ($y = 2$). Only structural parameters differ between the samples given in Table 1, with however very close Mt values. When the discharge time decreases, the lithium insertion capacity decrease is more important for the sample with a high Pr value.

3.2. Electrochemical characterisation upon cycling

An analysis of the shape of the first discharge I–U curves for every γ-Li_xMnO_2 samples (corresponding to the second discharge from starting γ-MnO_2 compounds) shows that the electrochemical behaviour of electrochemically prepared γ-Li_xMnO_2 compounds depends on the physico-chemical and structural parameters of the starting γ-MnO_2.

3.2.1. Influence of y on the voltage and intercalation capacity of γ-Li_xMnO_2

The electrochemical behavior of γ-Li_xMnO_2 materials obtained from starting γ-MnO_2 with different oxygen contents is illustrated in Fig. 4 which presents voltammograms of two materials with similar structural parameters. The position of peaks, associated with the 3 and 3.4 V phenomena, appears at a higher voltage as the oxygen content y increases. This effect is more marked for the first reduction peak, from 3.1 up to 3.4 V. Materials with

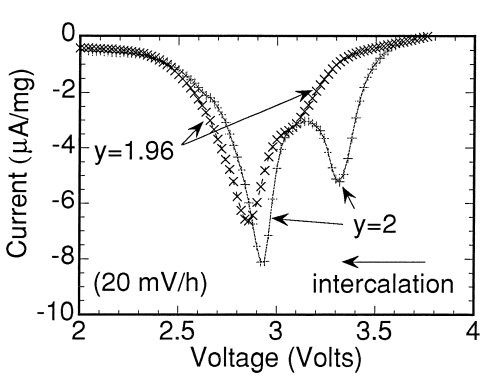

Fig. 4. Curves I–U of the first discharge for two different γ-Li_xMnO_2 compounds obtained from two different γ-MnO_2 with $y = 2$ and $y = 1.96$, in the 2–4 V range with a 20 mV/h scanning rate.

$y < 2$ exhibit a smaller capacity for the process at $U > 3$ V and then a smaller total Li insertion capacity.

3.2.2. Intercalation mechanism in γ-Li_xMnO_2

Opinions differ about the lithium intercalation mechanism in the γ-Li_xMnO_2 phase. Ohzuku et al. [4] claims that the lithium intercalation occurs in a single phase with typical NiAs structure. David et al. [5] also proposes an intercalation in a single lithiated phase, but corresponding to an intergrowth between a very distorted Ramsdellite type structure and spinel structure. Whilst Levi et al. [8] proposes a biphasic lithium intercalation process.

Informations about the intercalation mechanism were inferred from an analysis of the chrono-amperometric curves, as in the case of the γ-MnO_2/γ-Li_xMnO_2 transformation. A similar analysis was done for each phenomenon (3.4 and 3 V) in order to identify the kind of mechanism (mono or biphasic) during the intercalation, and for the case of a biphasic mechanism, the nature of the effect which limits the kinetics (diffusion in the forming phase or rate of displacement of the interphase zone).

Fig. 5 shows the second discharge curve from starting γ-MnO_2 with Pr = 45%, Mt = 8% and $y = 2$. The two redox phenomena show asymmetric peaks which are characteristic of a two-phase intercalation process [16]; this result is confirmed by X-ray diffraction experiments. For the first one at 3.4 V, a constant current is observed during each voltage step in the ascending part of the peak, indicating a kinetics limitation by the displacement rate of the interphase zone. On the other hand, at 3 V, the decreasing current observed during each voltage step in the ascending part of the peak indicates a limitation of the lithium diffusion through the new forming phase.

The second discharge curve from starting γ-MnO_2 with Pr = 95%, Mt = 3% and $y = 2$ was analyzed in the same way. The two redox phenomena correspond to transformations that operate by a two-phase mechanism, and in both cases (3.4 and 3 V), a limitation of the lithium diffusion through the new forming phase is observed.

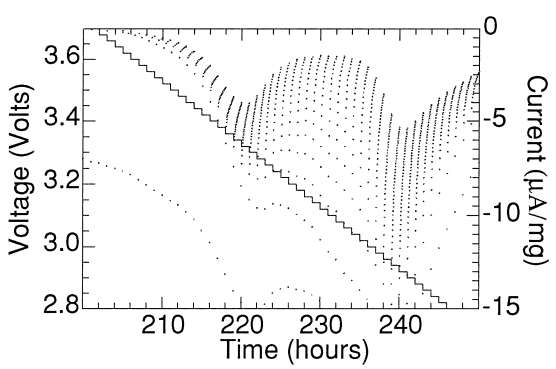

Fig. 5. Chrono-amperometric curves of the first lithium intercalation in γ-Li_xMnO_2 obtained from a γ-MnO_2 with Pr = 45%, Mt = 8% and $y = 2$, with a 20 mV/h scanning rate.

Table 2
Influence of time on the lithium insertion capacity for the second discharge of two HTMD samples

Pr, Mt of starting γ-MnO_2	Capacity (mA h/g)	
	Discharge in 6 h	Discharge in 100 h
45, 8	170	220
95, 3	132	200

3.2.3. Kinetics of the intercalation

The Pr influence on kinetics during the second discharge (for the same starting γ-MnO_2) was studied as mentioned above (during the first discharge) by examining the effect of a large change of discharge time on the lithium insertion capacity (Table 2). When the discharge time decreases, the lithium insertion capacity decrease is more important for the sample with a high Pr value. This result shows that Pr parameter also plays a role in the kinetics of reversible lithium intercalation in electrochemically formed γ-Li_xMnO_2.

3.3. Structural characterisation of γ-Li_xMnO_2

Structural characterization of materials at the end of the first discharge was carried out for two specific different cases:

a γ-MnO_2 material whose starting characteristics are quite similar to those of natural Ramsdellite: Pr = 45%, Mt = 8% and $y = 2$;

a γ-MnO_2 material whose starting characteristics are very close to those of Pyrolusite: Pr = 97%, Mt = 3% and $y = 2$.

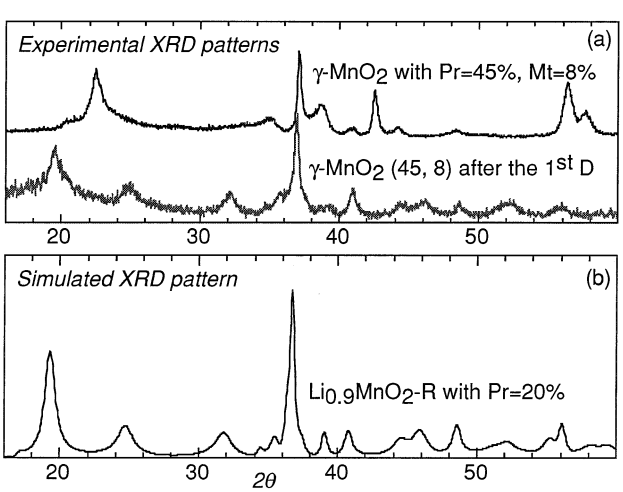

Fig. 6. (a) XRD patterns collected before and after the first lithium insertion into a γ-MnO_2 with Pr = 45%, Mt = 8% and $y = 2$. (b) XRD pattern calculated by simulating De Wolff defects in a γ-$Li_{0.9}MnO_2$ Ramsdellite type structure [11].

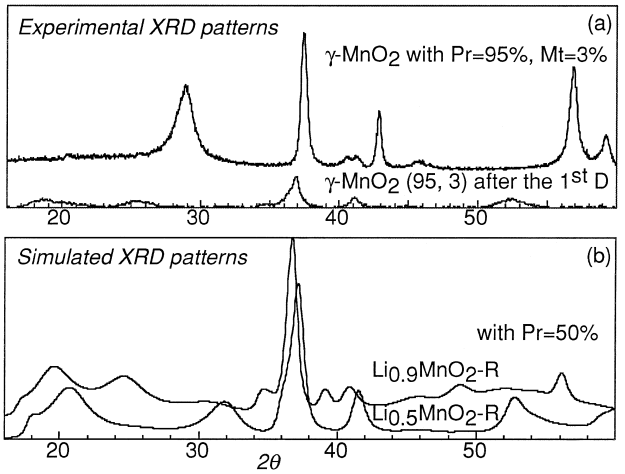

Fig. 7. (a) XRD patterns collected before and after the first lithium insertion in a γ-MnO_2 with Pr = 97%, Mt = 3% and $y = 2$. (b) XRD patterns calculated by simulating De Wolff defects in $Li_{0.5}MnO_2$ and $Li_{0.9}MnO_2$ Ramsdellite type structures [11].

3.3.1. Characterization of the γ-MnO_2 with Pr = 45%, Mt = 8% and y = 2, after the first lithium insertion

For the first case, Fig. 6a depicts the X-ray powder pattern before and after the first lithium insertion down to 2 V. A simulation of the X-ray diffraction pattern, taking into account the presence of de Wolff defects in a lithiated Ramsdellite, was calculated with the use of structural results taken in Ref. [11], for a Li content of 0.9 Li/Mn and Pr = 20% (Fig. 6b). It corresponds rather well with the experimental pattern. In agreement with HREM investigations, one can conclude that the γ-Li_xMnO_2 material at the end of the first discharge contains essentially a Ramsdellite structure, the defects being essentially of De wolff type. No other parameters allow to give some information about the evolution of microtwinning after the first lithium insertion.

3.3.2. Characterization of the γ-MnO_2 with Pr = 97%, Mt = 3% and y = 2, after the first lithium insertion

For the second case, a very poor crystallinity is observed at the end of the first discharge (Fig. 7a). Moreover, HREM studies do not show ordered structural domains within the lithiated compound. Both simulations (Fig. 7b) of X-ray diffraction patterns of γ-Li_xMnO_2, calculated with the use of structural results from Ref. [11] and taking into account a Pr value of 50%, give the best agreement with the experimental X-ray pattern. Hence, one can conclude that the structure is strongly modified, with probably an important decrease of the Pr value, and the appearance of other kinds of defects.

4. Conclusion

Electrochemical lithium insertion in γ-MnO_2 occurs via a two-phase mechanism leading to a new γ-Li_xMnO_2 phase similar to CDMO compounds. From an analysis of the electrochemical curves for various γ-MnO_2 samples, a nucleation and growth insertion process has been identified. The amount of inserted lithium, structural rearrangements and mechanism, during the lithium insertion, depend on characteristics (degree of active oxygen, structural parameters, etc.) of starting γ-MnO_2. The higher the Pr, the more important structural modifications should be, leading to a lower thermodynamic voltage and a slower first order transformation kinetic. The higher the degree of active oxygen, the larger the lithium content x. Comparisons of experimental and simulated X-ray diffraction patterns indicate a decrease of Pr upon the first electrochemical insertion in all γ-MnO_2 samples.

Electrochemical lithium intercalation in γ-Li_xMnO_2 occurs in two biphasic reversible steps. Their analysis reveals the predominant role of the characteristics of starting γ-MnO_2. γ-MnO_2 materials whose structure is quite similar to that of Pyrolusite are subjected to deep structural rearrangements with a kinetic of the lithium insertion limited by the lithium diffusion through the new forming phase, for both biphasic steps. Whilst those whose structure is quite close to that of Ramsdellite retain their structure with a kinetics of the lithium insertion limited by the displacement rate of the interphase zone for the first step at 3.4 V and the lithium diffusion for the second step at 3 V.

References

[1] Y. Chabre, J. Pannetier, Prog. Solid State Chem. 23 (1995) 1.
[2] S. Sarciaux, Thesis, Université de Nantes (France), January 1998.
[3] A. Verbaere, S. Sarciaux, A. Le Gal La Salle, D. Guyomard, Y. Piffard, to be published.
[4] T. Ohzuku, M. Kitagawa, T. Hirai, J. Electrochem. Soc. 136 (11) (1989) 3169.
[5] W.I.F. David, M.M. Thackeray, P.G. Bruce, J.B. Goodenough, Mater. Res. Bull. 19 (1984) 99.
[6] J.C. Nardi, J. Electrochem. Soc. 132 (8) (1985) 2556.
[7] Y. Shao-Horn, S.A. Hackney, B.C. Cornilsen, J. Electrochem. Soc. 144 (9) (1997) 3147.
[8] E. Levi, E. Zinigrad, H. Teller, M.D. Levi, D. Aurbach, E. Mengeritsky, E. Lester, P. Dan, E. Granot, H. Yamin, J. Electrochem. Soc. 144 (12) (1997) 4133.
[9] T. Nohma, T. Saito, N. Furukawa, H. Ikeda, J. Power Sources 26 (1989) 389.
[10] L. Li, G. Pistoia, Solid State Ionics 47 (1991) 241.
[11] M.M. Thackeray, M.H. Rossouw, R.J. Gummow, D.C. Liles, K. Pearce, A. De Kock, W.I.F. David, S. Hull, Electrochim. Acta 38 (9) (1993) 1259.
[12] T. Ohzuku, K. Sawai, T. Hirai, Chemical Express 4 (12) (1989) 777.
[13] M. Yoshio, H. Noguchi, T. Miyashita, H. Nakamura, A. Kozawa, J. Power Sources 54 (1995) 483.
[14] C. Mouget, Y. Chabre, Mac-Pile, Licensed from CNRS and UJF Grenoble to Bio-Logic, 1 av. de l'Europe, F-38640 Claix.
[15] J.M. Cowley, Diffraction Physics, New York, DIFFAX V1.76, 1990.
[16] D. Djurado, M. Barral, Y. Chabre, J.E. Fisher, Chemical Physics of Intercalation II, in: P. Bernier, et al. (Eds.), Plenum, New York, 1993, p. 255.